Journal of Instrumentation

Experimental ion mobility measurements in pure iC_4H_{10} and Ar-iC_4H_{10} mixtures

To cite this article: A.F.V. Cortez *et al* 2019 *JINST* **14** P04010

Jinst

Published by IOP Publishing for Sissa Medialab

Received: *December 5, 2018*
Revised: *March 1, 2019*
Accepted: *April 5, 2019*
Published: *April 17, 2019*

Experimental ion mobility measurements in pure iC_4H_{10} and Ar-iC_4H_{10} mixtures

A.F.V. Cortez,[a,b,1] **M.A.G. Santos,**[a,b] **R. Veenhof,**[c,d,e] **J. Escada,**[a] **P.N.B. Neves,**[f] **F.P. Santos,**[a,b] **C.A.N. Conde**[a,b] **and F.I.G.M. Borges**[a,b]

[a] *Laboratory of Instrumentation and Experimental Particle Physics — LIP, Rua Larga, 3004-516 Coimbra, Portugal*
[b] *Department of Physics, Faculty of Science and Technology, University of Coimbra, Rua Larga, 3004-516 Coimbra, Portugal*
[c] *National Research Nuclear University MEPhI, Kashirskoe Highway 31, Moscow, Russia*
[d] *CERN PH Department, Geneve 23, CH-1211 Switzerland*
[e] *Uludağ University, Faculty of Arts and Sciences, Physics Department, 16059 Bursa, Turkey*
[f] *Closer Consultoria, LDA, Av. Engenheiro Duarte Pacheco, Torre 2, 14º-C, Lisboa, 1070-102 Portugal*

E-mail: andre.f.cortez@gmail.com

Abstract: In this paper we present the results of the ion mobility measurements made in pure isobutane (iC_4H_{10}) and in mixtures with argon (Ar-iC_4H_{10}) for a total pressure of 8 Torr (10.6 mbar) and for low reduced electric fields in the 10 Td to 45 Td range (2.4–10.8 $kV{\cdot}cm^{-1}{\cdot}bar^{-1}$), at room temperature. The reduced mobilities, obtained from the peak centroid of the time-of-arrival spectra, are presented for Ar concentrations in the 5%–95% range.

Keywords: Charge transport and multiplication in gas; Gaseous detectors; Ion sources (positive ions, negative ions, electron cyclotron resonance (ECR), electron beam (EBIS)); Ionization and excitation processes

[1] Corresponding author.

https://doi.org/10.1088/1748-0221/14/04/P04010

2019 JINST 14 P04010

Contents

2019 JINST 14 P04010

1 Introduction

Over the last decade the knowledge of the different charge transport properties has gained renewed interest from the scientific community, namely for gases for radiation detectors, where it is essential in the modelling and in the understanding of their pulse shape formation [1–3]. This is specially relevant in detectors that include charge multiplication as a large number of ions is formed, and which can affect their performance. Examples include the Multi-Wire Proportional Chambers (MWPCs) [4], also of Transition Radiation Detectors (TRDs) [5, 6], where the electron and ion velocity influences their rate capability [5, 6] and of Time Projection Chambers (TPC) that have to deal with the space charge build-up from ion backflow at the endcaps [7]. For these cases the choice of the gas mixture, namely of the additives to the main gas (usually noble gases) implies the knowledge of several parameters of the gas mixture, among which the ions' mobility [3].

Argon is a common choice as main gas, while the additive is determined by the different operation parameters required by the multiple existing experiments and detectors used [3]. Recently, the LCTPC Collaboration has proposed a mixture of argon (Ar) with carbon-tetrafluoride (CF_4) eventually with the addition of isobutane (iC_4H_{10}) [7].

Thus, in the present work we study the impact in terms of ion mobility of increasing complex additive gases such as isobutane (iC_4H_{10}) in argon based mixtures. The total pressure used in this experiment was 8 Torr (10.6 mbar), while the reduced electric fields were those commonly used in gaseous detectors, thus extending previous studies developed in our group for other gases.

1.1 Ion mobility

When a group of ions moves in a gas atmosphere under the influence of an electric field, a simple relation between the ion drift velocity, v_d, and the applied electric field, E, can be defined:

$$K = \frac{v_d}{E} \tag{1.1}$$

where K is the ion mobility, usually expressed in units of $cm^2 \cdot V^{-1} \cdot s^{-1}$. In low uniform electric field conditions, these ions will eventually reach a steady state when the energy gained from the field

between collisions is below the thermal energy [8, 9] with the mobility reaching a constant value, as v_d becomes proportional to E. This is the case in the range of reduced electric fields studied in this work. To suppress the dependence of the mobility values on the gas pressure, K is usually expressed in terms of reduced mobility K_0:

$$K_0 = KN/N_0 \tag{1.2}$$

where N is the gas number density and N_0 is the Loschmidt number ($N_0 = 2.68678 \times 10^{19}$ cm^{-3} for 273.15 K and 101.325 kPa according to NIST [10]), being usually represented as a function of the reduced electric field, E/N, in units of Townsend (1 Td = 10^{-21} V·m^2).

When the electrostatic hard-core repulsion becomes negligible compared to the neutral polarization effect, which happens in the double limit of low E/N and low temperature, according to Langevin's theory [11] a limiting value for the ions' mobility can be estimated using the following equation,

$$K_{\text{pol}} = 13.88 \left(\frac{1}{\alpha\mu}\right)^{\frac{1}{2}} \tag{1.3}$$

where α is the neutral polarisability in cubic angstroms (α = 1.64±0.01 Å^3 for Ar [12] and α = 8.11±0.01 Å^3 for iC_4H_{10} [13]) and μ is the ion-neutral reduced mass in unified atomic mass units.

The Langevin limit can be used to calculate the low-field mobility at room temperature with relatively good accuracy [9], despite it was meant to low E/N and low temperature. It has nevertheless some known limitations in its application, for example with ions that undergo resonant charge transfer, with large molecules and atoms/molecules with low polarizability [14].

Moving to mixtures of several gases, a simple and useful way to predict the behaviour of ions is by using Blanc's law. Blanc found that the mobility of ions in gaseous mixtures, obeys a simple relationship which can be written as follows:

$$\frac{1}{K_{\text{mix}}} = \frac{f_1}{K_{\text{g1}}} + \frac{f_2}{K_{\text{g2}}} \tag{1.4}$$

where K_{mix} is the reduced mobility of the ion in the binary mixture; K_{g1} and K_{g2} the reduced mobility of that same ion in an atmosphere of 100% of gas #1 and #2 respectively; f_1 and f_2 are the molar fraction of each gas in the binary mixture [15].

As demonstrated in previous works, the combined use of these two concepts (Langevin polarization limit and Blanc's law) can also be very useful in the identification of the drifting ions. In such cases K_{g1} or K_{g2} in Blanc's law (equation (1.4)), can be obtained either using experimental values from literature or, when not existing, by using the Langevin limit formula (equation (1.3)), typically in cases of ions' drifting in gases other than the parent one.

2 Method and experimental setup

The mobility measurements presented in this study were obtained using the experimental system described in [16, 17]. Before each experiment the vessel is vacuum pumped down to pressures of 10^{-6} to 10^{-7} Torr. The measurements start with the flash of a UV flash lamp used to produce

2019 JINST 14 P04010

photoelectrons at CsI film deposited on the top of a Gas Electron Multiplier (GEM) [18] placed inside a gas vessel. The photoelectrons released from the CsI film are accelerated through the GEM holes by the electric field. These electrons will ionize the gas molecules, reproducing the charge multiplication mechanism in gas-filled detectors. While the resulting electrons are collected at the bottom of the GEM electrode, the cations formed will drift across a uniform electric field region towards a double grid where the signal will be produced. The reduced electric field (E/N) in the region between the Frisch and collecting grids is approximately one order of magnitude greater than the drift electric field. As a result, the collection efficiency of the ions is improved, allowing for a better signal without affecting significantly the ion mobility, as this distance corresponds to less than 1% of the total drift distance. The ions' charge signal collected in a pre-amplifier, is then fed to in a digital oscilloscope (Tektronix TDS 2022B), set to continuously average 128 pulses originating a time-of-arrival spectrum. To ensure minimal contamination, of the gas mixture by impurities due to outgassing processes, all the measurements were only taken when the signal stabilised, and all data taken in a 2–3 minutes time interval.

The system trigger is set by the flash of the UV flash lamp, providing the initial time information. The peaks in these time-of-arrival spectra are fitted to Gaussian curves, after the subtraction of the background (obtained without voltage in the GEM, i.e. without ions). Knowing the average drift time of these ions in a known distance (4.273 cm), taken from the peaks' centroid, the drift velocity can be determined, and the mobility can then be found using equation (1.1).

Although the present experimental system does not allow for a direct identification, the fact that the present system relies on a GEM allows to control the maximum energy of the electrons helps in the primary ion identification. With the primary ions identified, following the possible secondary reaction paths allows a reliable identification of the detected ions in most cases.

Even though the measurements are performed at low pressure (up to a few tens of Torr) the results have been consistent with data obtained at higher pressures [14, 19, 20]. Nonetheless, it must be stressed out that the obtained mobility of the ions observed may depend on the time evolution of relative abundance of the ions, as it is determined by the gas pressure and drift distance. If the reaction times (pressure dependent) involved in the formation of the ions observed are much shorter than the drift time, the ion mobility measured will not be affected by the pressure. This happens because the reactions will be completed shortly after the primary ion formation. Instead, if the reaction times involved are of the order of magnitude of the drift time, the obtained mobility of the final ions will be affected. In such cases, choosing an adequate pressure reduced distance (*pressure*×*drift distance*), the influence of the pressure can be compensated by choosing an adequate drift distance, which will result in a similar relative abundance of the final ions. Still, working at low pressure presents several advantages with the most significant one being related with the possibility of studying in more detail the fundamental processes involved in the ion transport while allowing to reduce the overall cost of the experiment.

3 Results and discussion

The mobility of the ions originated in pure iC_4H_{10} and in Ar-iC_4H_{10} mixtures has been measured for reduced electric fields E/N in the 10 to 45 Td range and 8 Torr pressure, at room temperature (293 K). The range of E/N values considered in this work is within the conditions of low reduced field.

2019 JINST 14 P04010

3.1 Argon (Ar)

As reported in a previous work [16], in pure Ar two different types of ions are observed for electron impact ionization with energies of about 20 eV: the atomic and the dimer rare gas ions. While the atomic ion (Ar^+) is a direct result of electron impact ionization (equation (3.1)), the dimer ion (Ar_2^+) is, even at our working pressures, the result of three-body collision between Ar^+ and two neutrals. Their formation process can be described by the following reactions.

$$Ar + e^- \rightarrow Ar^+ + 2e^- \tag{3.1}$$

$$Ar^+ + 2Ar \rightarrow Ar_2^+ + Ar \tag{3.2}$$

The atomic ion has a lower mobility than the dimer one, due to resonant charge transfer process between Ar^+ ions and Ar atoms, which results in the slowing down of these ions.

Table 1. Ionization products, ionization cross sections for electron impact (25 eV) on Ar [21], appearance energy (A.E.) [22] and respective reaction rates.

Reaction	Cross Sec. (10^{-16}cm^2)	A. E. (eV)	Rate Const.	Ref.
$e^- + Ar \rightarrow Ar^+ + 2e^-$	1.24	15.70	—	[21, 22]
$Ar^+ + Ar \rightarrow Ar + Ar^+$	—	—	4.6×10^{-10} cm$^3\cdot$s^{-1}	[14]
$Ar^+ + 2Ar \rightarrow Ar_2^+ + Ar$	—	—	2.2×10^{-31}cm$^6\cdot$s^{-1}	[23]

3.2 Isobutane (iC_4H_{10})

Butane, C_4H_{10}, is the general designation for two different compounds with the same formula but different structures: unbranched and branched, respectively n-butane and isobutane. This difference in the structure, can originate different physical and chemical properties. However, the data required in this work (reaction rates, cross sections, appearance energies, product distributions) is similar enough for both structures [24]; so whenever data is not available for isobutane, the one for butane will be used.

In pure isobutane (iC_4H_{10}), the mobilities of the ions in the parent gas were measured for different reduced electric fields E/N (10–45 Td) and for a pressure of 8 Torr at room temperature (293 K), for a constant V_{GEM} of 25 V.

Two peaks were observed between 10 and 40 Td. A typical example of a time-of-arrival spectrum at a pressure of 8 Torr, a reduced electric field of 15 Td and voltage across the GEM, V_{GEM}, of 25 V, is shown in figure 1.

As said before, primary ion identification is very important in our work, as the current method does not provide direct identification. As already mentioned, fixing the GEM voltage allows to identify the primary ions produced in the GEM holes and, knowing their possible reaction channels, will ultimately allow to identify the final ions.

In table 2, the possible reactions resulting from electron impact in iC_4H_{10} for electron energies of 25 eV, together with the appearance energies and their product distribution of the different ions are summarized. The probabilities indicated for the product distribution were estimated from data in [25].

2019 JINST 14 P04010

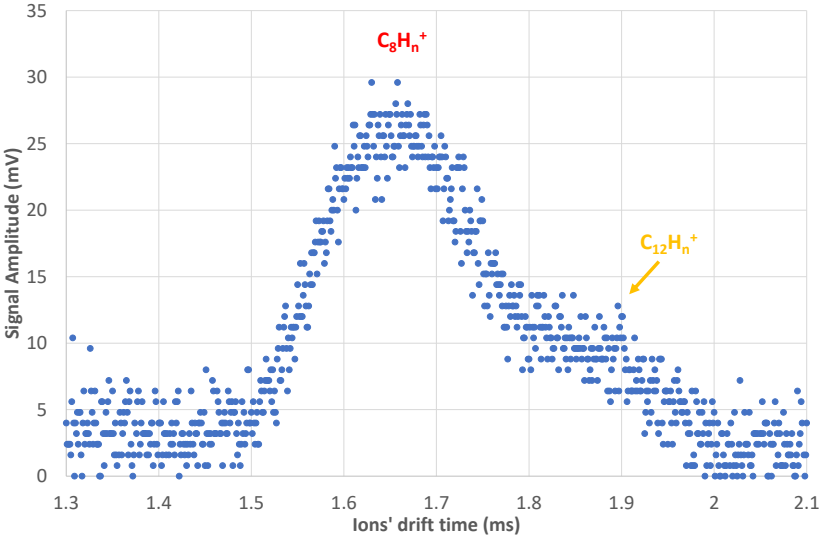

Figure 1. Time-of-arrival spectrum averaged over 128 pulses for pure iC_4H_{10} at a pressure of 8 torr, temperature of 293 K and a reduced electric field of 15 Td, with a voltage across GEM of 25 V.

Table 2. Ionization products, appearance energies (A. E.) for ions formed in C_4H_{10} and the expected product distribution in iC_4H_{10} for electron impact ionization at 25 eV [25].

Reaction	A. E. (eV)	Prod. Dist.
$e^- + iC_4H_{10} \rightarrow C_2H_3^+ + C_2H_6 + H + 2e^-$	—	11.3 %
$e^- + iC_4H_{10} \rightarrow C_2H_5^+ + C_2H_5 + 2e^-$	13.80	2.7 %
$e^- + iC_4H_{10} \rightarrow C_3H_5^+ + CH_4 + H + 2e^-$	14.55	23.1 %
$e^- + iC_4H_{10} \rightarrow C_3H_6^+ + CH_4 + 2e^-$	10.88	14.6 %
$e^- + iC_4H_{10} \rightarrow C_3H_7^+ + CH_3 + 2e^-$	11.16	45.6 %
$e^- + iC_4H_{10} \rightarrow C_4H_9^+ + H + 2e^-$	11.60	1.7 %
$e^- + iC_4H_{10} \rightarrow C_4H_{10}^+ + 2e^-$	10.23	1.0 %

Table 2 shows that there are three groups of ions produced inside the GEM holes: a group with 2 carbons ($C_2H_3^+$, $C_2H_4^+$ and $C_2H_5^+$) that corresponds to 14% of the primary ions, a group with 3 carbons ($C_3H_3^+$, $C_3H_5^+$, $C_3H_6^+$ and $C_3H_7^+$) corresponding to about 83.3% of the ions formed and a 4-carbon ion group ($C_4H_9^+$ and $C_4H_{10}^+$) that corresponds to about 2.7%.

The primary ions formed may further react with neutrals, leading to the formation of a ternary structure of $C_4H_9^+$ and $C_4H_{10}^+$ [26], as shown in table 3, where the possible reactions involving the primary ions and C_4H_{10} molecules, together with their respective rate constants and product distributions are summarized [24]. Data used here is for C_4H_{10}, as mentioned before, reaction rates do not vary significantly from C_4H_{10} to iC_4H_{10} [24].

As can be seen in table 3, the primary ions will, in a first stage, lead to 4-carbon ions in C_4H_{10}, through fast reactions with reaction rates of the order of 10^{-9} $cm^3 \cdot s^{-1}$. Thus, it is expected, that for very low pressures (corresponding to a lower number of collisions), these will be the ions appearing

2019 JINST 14 P04010

Table 3. Ionization products from secondary reactions with the respective reaction rates and product distribution in butane (C_4H_{10}) [26, 27].

Reaction	Rate Const. ($cm^3 \cdot s^{-1}$)	Prod. Dist.
$C_2H_3^+ + C_4H_{10} \rightarrow C_3H_7^+ + C_3H_6$	1.3×10^{-9}	35 %
$C_2H_3^+ + C_4H_{10} \rightarrow C_4H_9^+ + C_2H_4$	1.3×10^{-9}	65 %
$C_2H_5^+ + C_4H_{10} \rightarrow C_4H_9^+ + C_2H_6$	1.0×10^{-9}	100 %
$C_3H_5^+ + C_4H_{10} \rightarrow C_4H_9^+ + C_3H_6$	0.45×10^{-9}	100 %
$C_3H_6^+ + C_4H_{10} \rightarrow C_4H_8^+ + C_3H_8$	0.78×10^{-9}	93 %
$C_3H_6^+ + C_4H_{10} \rightarrow C_4H_9^+ + C_3H_7$	0.78×10^{-9}	7 %
$C_3H_7^+ + C_4H_{10} \rightarrow C_4H_9^+ + C_3H_8$	0.37×10^{-9}	100 %
$C_4H_9^+ + C_4H_{10} \rightarrow C_8H_{17}^+ + H_2$	4.7×10^{-14}	100 %
$C_4H_{10}^+ + C_4H_{10} \rightarrow C_8H_{18}^+ + H_2$	4.2×10^{-14}	100 %
$C_8H_{17}^+ + C_4H_{10} \rightarrow C_{12}H_{25}^+ + H_2$	0.28×10^{-14}	100 %
$C_8H_{18}^+ + C_4H_{10} \rightarrow C_{12}H_{26}^+ + H_2$	0.30×10^{-14}	100 %

in the drift spectra. However, for higher pressures, these ions may undergo further reactions, which are much slower, with reaction rates about five orders of magnitude lower (about 10^{-14} $cm^3 \cdot s^{-1}$) than the first quicker ones, that will lead to the formation of much heavier molecular ions: from a 8-carbon ion group ($C_8H_{17}^+$ and $C_8H_{18}^+$) to a 12-carbon ion group ($C_{12}H_{25}^+$ and $C_{12}H_{26}^+$), in a third stage [26].

Figure 2 shows the reduced ion mobility as a function of the reduced electric field in the 10 to 45 Td range, at 8 Torr, with a V_{GEM} of 25 V and at room temperature, together with the Langevin limit ($E/N \rightarrow 0$ Td) for the ions expected to be present in pure iC_4H_{10}. At 45 Td, only one peak is observed because the higher electric field leads to a drift time that is much shorter than the required for the sequence of reactions required to the formation of $C_{12}H_n^+$.

At the lowest studied reduced electric field, 10 Td, the measured mobility is of about $0.60\,cm^2 \cdot V^{-1} \cdot s^{-1}$ for the heavier ion, identified as $C_{12}H_n^+$, and $0.65\,cm^2 \cdot V^{-1} \cdot s^{-1}$ for the lighter ion, expected to be $C_8H_n^+$. As can be seen in figure 2, the mobilities obtained for this E/N have a deviation of about 20% from those obtained from Langevin theory. However, this result is not surprising since Langevin theory seems to fail when predicting the mobility of massive ions [14]. Still, when comparing our results for low reduced electric fields with the ones found in literature, we find that our results are in good agreement with the ones obtained by other authors [19, 28] at atmospheric pressure, with a small deviation of less than 2% for $C_{12}H_n^+$ even though, at our pressures, $C_{12}H_n^+$ mobility is expected to be affected by its predecessor ion. The fact that the mobilities of $C_8H_n^+$ and $C_{12}H_n^+$ are not significantly different may hint the reason why that the deviation observed is small.

However, regarding the relative abundance of the ions observed at low pressure, it is important to stress that it may differ from those obtained at higher pressures as the reactions involved in the

2019 JINST 14 P04010

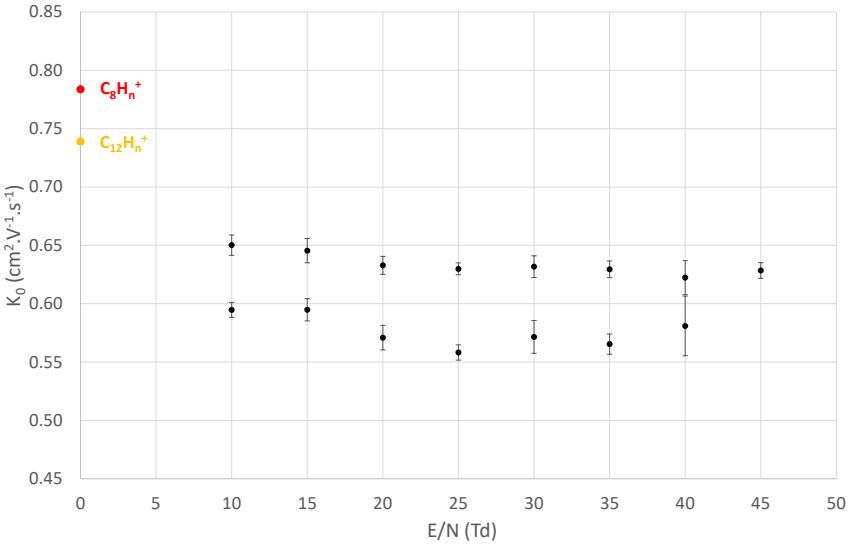

Figure 2. Reduced mobility of the ions produced in iC_4H_{10} for a pressure range of 6-10 Torr and for E/N vales in the range 10-45 Td range. The Langevin polarization limits for $C_8H_n^+$ (red) and $C_{12}H_n^+$ (orange) ions are also represented. Error bars represent the standard deviation of the experimental measurements.

formation of the heavier ions will be completed faster than at lower pressures. Still, in this case, no significant variation is expected on the mobility of ions with pressure if the reaction times involved are much shorter than the ions' drift time, as discussed before.

3.3 Argon-isobutane (Ar-iC_4H_{10}) mixture

Figure 3 presents several time-of-arrival spectra for different argon-isobutane (Ar-iC_4H_{10}) mixtures (5%, 80%, 85% and 95% of Ar), for a total pressure of 8 Torr, using a V_{GEM} of 25 V and a reduced electric drift field of 15 Td, at room temperature. As can be seen, the number and mobility of peaks in the drift spectra is seen to change.

The primary ions originated in the mixture are expected to be the same as in pure iC_4H_{10} since the ionization potential of Ar (15.82 eV [22]) is much higher than that of iC_4H_{10} (10.74 eV [25]). From the total electron impact ionization cross-sections for Ar and iC_4H_{10} and energies up to 25 eV, only for high Ar concentrations (above 82%) is the formation of Ar primary ions favoured. Nevertheless, a charge transfer reaction between Ar ions and iC_4H_{10} is expected to occur, since it this process is energetically favoured. Although charge transfer rates between Ar^+ and iC_4H_{10} could not be found in the literature, it was assumed that they are similar to those between Ar^+ and C_4H_{10} (k=1.4×10^{-9} cm^3·s^{-1}). Table 4 presents the possible reactions between Ar^+ and C_4H_{10} and the corresponding product distribution.

From table 4, it is expected that the presence of Ar^+ ions will lead to the formation of the same ions as in pure iC_4H_{10}. However, whether the primary ion is Ar^+ or an iC_4H_{10} ion can affect the final ion distribution and can explain the evolution of the time spectra for these mixtures with increasing Ar concentration, as seen in figure 3. In fact, the increasing Ar concentration in the mixture implies an increase in the overall reaction time needed to form the heavier ions, as charge transfer is one additional step required during drift time. This may imply that the abundance of heavier clusters will depend on the overall pressure if the distance is kept constant.

2019 JINST 14 P04010

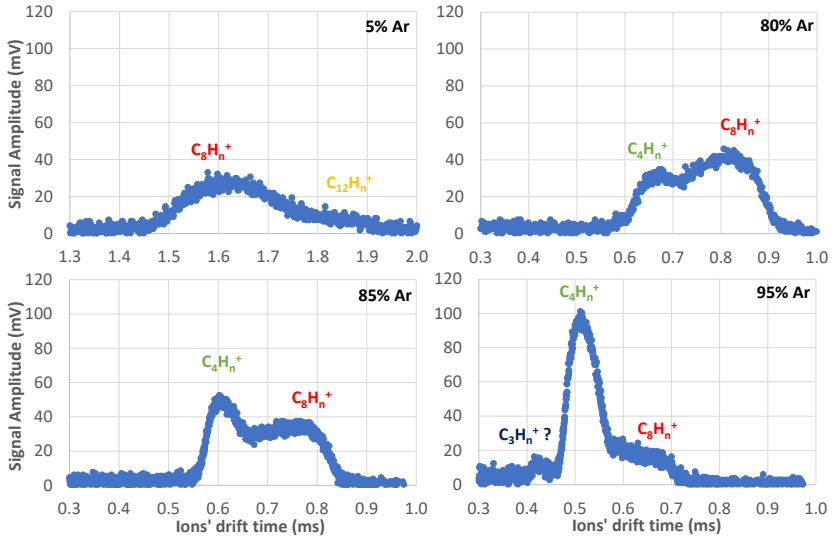

Figure 3. Time-of-arrival spectra (average of 128 pulses) recorded for several Ar-iC_4H_{10} mixtures (5%, 80%, 85% and 95% of Ar) at total pressure of 8 torr, reduced electric field of 15 Td, V_{GEM} of 25 V and room temperature (293 K).

Table 4. Ionization products and respective reaction rates and product distribution for the charge transfer reactions between argon ions (Ar^+) and butane (C_4H_{10}) [27].

Reaction	Rate Const. ($cm^3 \cdot s^{-1}$)	Prod. Dist.
$Ar^+ + C_4H_{10} \rightarrow C_2H_3^+ + C_2H_6 + H + Ar$		27 %
$Ar^+ + C_4H_{10} \rightarrow C_2H_4^+ + C_2H_6 + Ar$		8 %
$Ar^+ + C_4H_{10} \rightarrow C_2H_5^+ + C_2H_5 + Ar$	1.4×10^{-9}	32 %
$Ar^+ + C_4H_{10} \rightarrow C_3H_5^+ + CH_4 + H + Ar$		26 %
$Ar^+ + C_4H_{10} \rightarrow C_3H_7^+ + CH_3 + Ar$		5 %
$Ar^+ + C_4H_{10} \rightarrow C_4H_9^+ + H + Ar$		2 %

Analysing figure 3, it can be seen that with increasing Ar concentration, the drift time of the ions decreases as well as the abundance of heavier ions formed. The much lower polarizability and mass of Ar, as compared to iC_4H_{10} (α and μ in Langevin formula — eq. (1.3)) results in a decrease in drift time which, together with the additional step required (charge transfer from Ar^+ to iC_4H_{10}), will also affect the formation of heavier ions.

To confirm the identification of the ions originating the peaks in the different spectra we used Blanc's law. Figure 4 shows the measured values of the reduced mobility for the ions produced in the different Ar-iC_4H_{10} mixtures in the pressure range of 6–10 Torr, and for E/N of 15 Td at room temperature. In the same figure, Blanc's law prediction is also represented for two of the main candidate ions — $C_4H_n^+$ (green), $C_8H_n^+$ (red). In this case, Blanc's law theoretical curve for $C_{12}H_n^+$ ions is not shown as the obtained mobility of these ions will be highly affected by its predecessor ions. K_{g1} and K_{g2} in Blanc's law (equation (1.4)) were obtained either using our experimental

2019 JINST 14 P04010

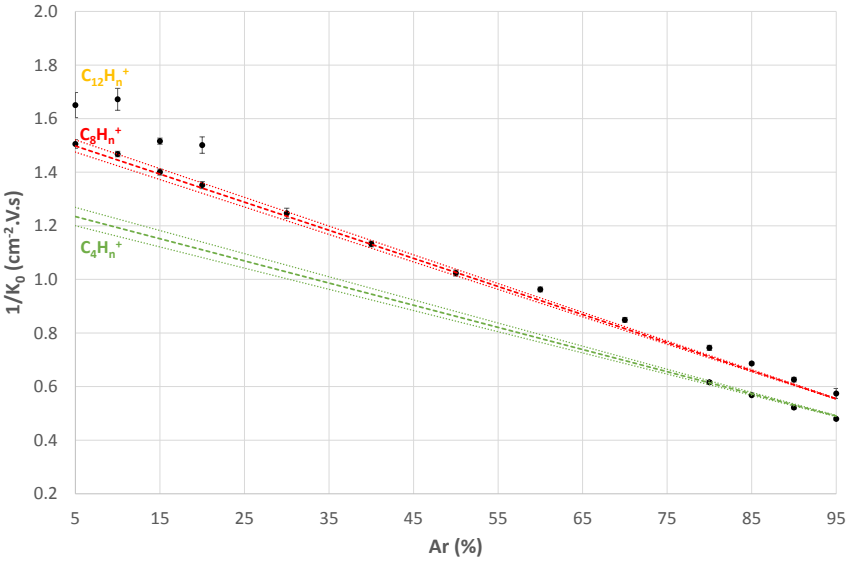

Figure 4. Reduced mobility of the ions produced in the Ar-iC_4H_{10} mixture for a pressure of 8 Torr and E/N of 15 Td at room temperature. The dashed lines represent the mobility values expected from Blanc's law for $C_4H_n^+$ (green) and $C_8H_n^+$ (red), while the dotted lines represent the respective uncertainty. Error bars represent the standard deviation of the experimental measurements.

values or using the Langevin polarization limit formula (equation (1.3)). In the case of the mobility of these ions in pure Ar the Langevin's formula (equation (1.3)) was used as it describes correctly the mobility behaviour of ions moving in Ar [14]. For ions drifting in pure iC_4H_{10} two different approaches were used. In the case of $C_8H_n^+$ our experimental values were used, since the reactions are much faster than the drift times involved, not influencing the overall mobility of this ion. In the case of $C_4H_n^+$, which is not present in the time spectra since it undergoes fast reactions that will transform it into $C_8H_n^+$ ions, we used the Langevin polarization limit formula. Since the Langevin polarization limit has some limitations for large molecules, as it is the case of iC_4H_{10}, a correction to this limit, already used in [14, 29], was introduced in the displayed values.

As seen in figure 4 from pure iC_4H_{10} to 20% Ar, two peaks can be observed. Since $C_{12}H_n^+$ ions (lower mobility peak) is highly affected by its predecessor ion not much can be said about its Blanc's law compliance. As for the peak with higher mobility, $C_8H_n^+$, it is possible to see that the experimental mobility values of this group of ions follow closely the theoretical ones. As Ar concentration is increased from 20% to 80% Ar, only one peak can be seen in the time-of-arrival spectra. We believe that the ion observed is $C_8H_n^+$ as the formation of $C_{12}H_n^+$ requires one further slow step for its formation and, with increasing Ar concentration, the ion drift time tends to decrease, not allowing the needed time for the slower reactions leading to $C_{12}H_n^+$ to be completed during the drift time, as already discussed.

Further increasing Ar concentration (above 80% Ar) leads to the appearance of a new peak with even higher mobility at the left of $C_8H_n^+$, as seen in figure 3. The ions responsible for this new peak are thought to be $C_4H_n^+$, either coming from the primary ions ($C_4H_8^+$, $C_4H_9^+$ and $C_4H_{10}^+$) or resulting from the fast secondary reactions (tables 3, 4 and 5), that do not enough time during their drift to convert into $C_8H_n^+$, since the partial pressure of is small. This assumption is in accordance

2019 JINST 14 P04010

with Blanc's law. The observed behaviour is a direct consequence of the decrease in the drift time linked to the high Ar concentration. Also, it is important to stress that increasing E/N will further shorten the drift times, preventing the formation of more complex ion species.

Table 5 summarizes the results obtained. The mobilities observed for the heavier ion, $C_{12}H_n^+$, should be seen as an upper limit, as its mobility is expected to be affected by its predecessor ion, $C_8H_n^+$, as the reactions leading to its formation are slow compared to the drift time.

Table 5. Mobility of the peaks observed for the Ar-iC_4H_{10} mixture ratios studied, obtained for E/N of 15 Td, a pressure of 8 Torr at room temperature (293 K). The mobilities observed for the heavier ion, $C_{12}H_n^+$, should be seen as an upper limit as its mobility is expected to be affected by its predecessor ion, $C_8H_n^+$, as the reactions leading to its formation are slow.

Ar-iC_4H_{10} mixture	Mobility ($cm^2 \cdot V^{-1} \cdot s^{-1}$)		
(% of Ar)	$C_4H_n^+$	$C_8H_n^+$	$C_{12}H_n^+$
5%	—	0.664 ± 0.007	0.606 ± 0.017
10%	—	0.681 ± 0.005	0.598 ± 0.015
15%	—	0.714 ± 0.006	0.660 ± 0.009
20%	—	0.740 ± 0.007	0.666 ± 0.014
30%	—	0.802 ± 0.012	—
40%	—	0.883 ± 0.008	—
50%	—	0.977 ± 0.011	—
60%	—	1.039 ± 0.010	—
70%	—	1.178 ± 0.013	—
80%	1.623 ± 0.017	1.343 ± 0.017	—
85%	1.762 ± 0.013	1.458 ± 0.011	—
90%	1.915 ± 0.021	1.597 ± 0.022	—
95%	2.084 ± 0.023	1.742 ± 0.056	—

The fact that the mobility behaviour obtained at low pressure is close to the one expected at higher pressures (close to the atmospheric one), is related to the fact that these values (both at low and high pressure) are close, even though the reaction time is of the order of magnitude of the drift time at our experimental conditions (about 8 Torr).

4 Conclusion

In the present work we measured the reduced mobility of ions originated by electron impact for electron energies up to 25 eV, in pure iC_4H_{10} and Ar-iC_4H_{10} mixtures for pressures from 6 to 10 Torr, low reduced electric fields from 10 to 45 Td and different mixture ratios (from 0 to 100% Ar).

In pure iC_4H_{10}, two peaks were observed from 5 Td up to 40 Td, which were attributed to $C_8H_n^+$ and $C_{12}H_n^+$. Increasing E/N to 45 Td, only one peak was observed ($C_8H_n^+$) as a result of the decreasing drift time which does not allow the formation of more complex and heavier ions

2019 JINST 14 P04010

(requiring additional slower reactions) to be formed. The mobility values obtained in this case are consistent with the ones obtained by other authors, although not quite agreeing with Langevin's limit.

In Ar-iC_4H_{10} mixtures, depending on the relative abundance of the gases, different ions with different abundances may appear. For concentrations ranging from pure iC_4H_{10} up to 20% Ar, the mobility values obtained for the different peaks observed are consistent with both $C_8H_n^+$ (higher mobility) and $C_{12}H_n^+$ (lower mobility). Increasing Ar concentration up to 70%, only one peak remains, thought to be due to $C_8H_n^+$ ions. Above this concentration a new peak of even higher mobility appears. This peak is expected to be from $C_4H_n^+$ ions. The change in the nature or abundance of the ions present in the different mixtures, favouring the lower mass ions, is due to the increasing number of slower reactions required in the heavier ion formation, and the lower drift times at increasing Ar concentrations or E/N. This implies that reactions for the formation of the more complex ions will not be complete (as seen at 45 Td in pure iC_4H_{10}), with the ions observed displaying the expected mobility of the ions with lower mass.

The experimental mobility values are in good agreement with the theoretical values given by Blanc's law. In addition, the experimental results did not display a significant dependence over the range of E/N studied (10–45 Td). Future work is expected with other gaseous mixtures. It is our intention to proceed this line of investigation using different mixtures of Ar, CF_4, CH_4, C_2H_6 and iC_4H_{10} that will help to understand ternary gas mixtures of interest for the LCTPC Collaboration of the International Linear Collider (ILC) experiment such as Ar-CF_4-CH_4, Ar-CF_4-C_2H_6 and Ar-CF_4-iC_4H_{10}.

Acknowledgments

We would like to thank Paul Colas (CEA Saclay) and Jochen Kaminski (Univ. Bonn) for their genuine interest on this subject which motivated this work. This work was supported by the RD51 Collaboration/CERN, through the common project "Measurement and calculation of ion mobility of some gas mixtures of interest". André F.V. Cortez received a PhD scholarship from FCT-Fundação para a Ciência e Tecnologia (SFRH/BD/52333/2013).

References

[1] W. Blum and L. Rolandi, *Particle Detection with Drift Chambers*, Springer-Verlag, Berlin, Germany, (1994).

[2] G.F. Knoll, *Radiation detection and measurements*, John Wiley and Sons, Inc., New York, U.S.A., (2000).

[3] F. Sauli, *Gaseous Radiation Detectors: Fundamentals and Applications*, Cambridge Monographs on Particle Physics, Nuclear Physics and Cosmology, Cambridge University Press, (2014).

[4] A. Andronic, C. Garabatos, D. Gonzalez-Diaz, A. Kalweit and F. Uhlig, *A Comprehensive study of rate capability in Multi-Wire Proportional Chambers*, 2009 *JINST* **4** P10014 [arXiv:0909.0242].

[5] B. Dolgoshein, *Transition radiation detectors*, *Nucl. Instrum. Meth.* **A 326** (1993) 434.

[6] A. Andronic and J.P. Wessels, *Transition radiation detectors*, *Nucl. Instrum. Meth.* **A 666** (2012) 130 [arXiv:1111.4188].

2019 JINST 14 P04010

[7] LCTPC collaboration, *A Time Projection Chamber with GEM-Based Readout*, *Nucl. Instrum. Meth.* **A 856** (2017) 109 [arXiv:1604.00935].

[8] G.A. Eiceman, Z. Karpas and H.H.J. Hill, *Ion Mobility Spectrometry*, third ed., CRC Press — Taylor & Francis Group, (2014).

[9] E.W. McDaniel, J.B.A. Mitchell and M.E. Rudd, *Atomic collisions — heavy particle projectiles*, Wiley, (1993), p. 498.

[10] National Institute of Standards and Technology, Gaithersburg, Maryland, 20899-8320, http://physics.nist.gov/cuu/Constants/Table/allascii.txt.

[11] P. Langevin, *Une formule fondamentale de théorie cinetique*, *Annal. Chimie Physique* **5** (1905) 245.

[12] R.R. Teachout and R.T. Pack, *The static dipole polarizabilities of all the neutral atoms in their ground states*, *Atom. Data Nucl. Data Tabl.* **3** (1971) 195.

[13] C.C.J.O. Hirschfelder and R. Bird, *Molecular Theory of Gases and Liquids. Fundamental information on molecular polarizabilities*, John Wiley and Son, Inc., New York, U.S.A., (1954).

[14] Y. Kalkan, M. Arslandok, A.F.V. Cortez, Y. Kaya, I. Tapan and R. Veenhof, *Cluster ions in gas-based detectors*, 2015 *JINST* **10** P07004.

[15] A. Blanc, *Recherches sur le mobilités des ions dans les gaz*, *J. Phys. Theor. Appl.* **7** (1908) 825.

[16] P.N.B. Neves, C.A.N. Conde and L.M.N. Távora, *Experimental measurement of the mobilities of atomic and dimer Ar, Kr and Xe ions in their parent gases*, *J. Chem. Phys.* **133** (2010) 124316.

[17] A.F.V. Cortez et al., *Experimental ion mobility measurements in Ne-N_2*, 2016 *JINST* **11** P11019.

[18] F. Sauli, *GEM: A new concept for electron amplification in gas detectors*, *Nucl. Instrum. Meth.* **A 386** (1997) 531.

[19] G. Schultz, G. Charpak, F. Sauli, *Mobilities of positive ions in some gas mixtures used in proportional and drift chambers*, *Rev. Phys. Appl.* **3171** (1977) 67.

[20] A. Deisting, C. Garabatos and A. Szabo, *Ion mobility measurements in Ar-CO_2, Ne-CO_2, and Ne-CO_2-N_2 mixtures, and the effect of water contents*, *Nucl. Instrum. Meth.* **A 904** (2018) 1 [arXiv:1804.10288].

[21] R. Rejoub, B.G. Lindsay and R.F. Stebblings, *Determination of the absolute partial and total cross sections for electron-impact ionization of the rare gases*, *Phys. Rev.* **A 65** (2002) 042713.

[22] B. Gstir et al., *Electron impact multiple ionization of neon, argon and xenon atoms close to threshold:appearance energies and Wannier exponents*, *J. Phys.* **B 35** (2002) 2993.

[23] K. Hiraoka and T. Mori, *Formation and stabilities of cluster ions Ar_n^+*, *J. Chem. Phys.* **90** (1989) 7143.

[24] M.S.B. Munson, *Effects of structure on the reactions of hydrocarbon ions*, *J. Phys. Chem.* **71** (1967) 3966.

[25] I. Omura, *Mass spectra at low ionizing voltage and bond dissociation energies of molecular ions from hydrocarbons*, *Bull. Chem. Soc. Jpn.* **34** (1961) 1227.

[26] R. Neagu-Plesu, J.A. Herman and A.G. Harrison, *Ion/molecule reactions in isobutane near the ionization threshold*, *Rapid Commun. Mass Spectrom.* **1** (1987) 63.

[27] C.Q. Jiao, C.A. DeJoseph Jr. and A. Garscadden, *Electron impact ionization and ion reactions in n-butane*, *J. Phys.* **D 40** (2007) 409.

[28] T. Yamashita et al., *Measurements of electron drift velocities and positive ion mobilities for gases containing CF-4. 2.*, *Nucl. Instrum. Meth.* **A 317** (1992) 213.

[29] A.F.V. Cortez, *Novel Techniques for High Pressure Noble Gas Radiation Detectors*, Ph.D. Thesis, University of Coimbra, Portugal, (2018).

2019 JINST 14 P04010